A constrained model predictive wind farm controller providing active power control An LES study

Boersma, Sjoerd; Rostampour, Vahab; Doekemeijer, Bart; Van Geest, Will; Van Wingerden, Jan Willem

DOI
10.1088/1742-6596/1037/3/032023

Publication date
2018

Document Version
Final published version

Published in
Journal of Physics: Conference Series

A constrained model predictive wind farm controller providing active power control: an LES study

IOP Conf. Series: Journal of Physics: Conf. Series **1037** (2018) 032023 doi:10.1088/1742-6596/1037/3/032023

A constrained model predictive wind farm controller providing active power control: an LES study

Sjoerd Boersma, Vahab Rostampour, Bart Doekemeijer, Will van Geest, Jan-Willem van Wingerden

Delft Center of Systems and Control, Delft University of Technology, The Netherlands

E-mail: S.Boersma@tudelft.nl

Abstract. The objective of active power control in wind farms is to provide ancillary grid services. Improving this is vital for a smooth wind energy penetration in the energy market. One of these services is to track a power reference signal with a wind farm by dynamically de- and uprating the turbines. In this paper we present a computationally efficient model predictive controller (MPC) for computing optimal control signals for each time step. It is applied in the PArallelized Large-eddy simulation Model (PALM), which is considered as the real wind farm in this paper. By taking measurements from the PALM, we show that the closed-loop controller can provide power reference tracking while minimizing variations in the axial forces by solving a constrained optimization problem at each time step. A six turbine simulation case study is presented in which the controller operates with optimised turbine yaw settings. We show that with these optimized yaw settings, it is possible to track a power signal that temporarily exceeds the power harvested when operating under averaged greedy control turbine settings. Additionally, variations in the turbine's force signals are studied under different controller settings.

1. Introduction

The trend towards clean energy is irreversible [1]. A large part of this clean energy finds its origin in wind, making the stimulation of wind power penetration in the energy market important. One bottleneck in this process is the provision of grid facilities such as secondary frequency regulation by wind farms. Here, the objective is to have the wind farm's power generation track a certain demanded power signal generated by transmission system operators (TSOs), during a time span of several minutes [2]. In wind farms, this objective could be separated into two tasks: 1) distribution of the wind farm power reference signal to reference signals for the individual turbines in the farm and 2) tracking of the local references by the individual turbines. Two common actuation methods to ensure tracking are axial induction and wake redirection control [3]. An example of axial induction actuation is [4] in which both the distribution and tracking task are solved using a wind farm controller, which solves a constrained optimization problem containing wake and turbine models. In [5], no wake model nor constraints have been taken into account in the controller providing tracking and an uniform reference distribution mechanism is employed. Other wind farm controllers providing power tracking using axial induction actuation are presented in [6–9]. The latter controllers are however not tested in a high-fidelity simulation environment making it difficult to assess if the therein presented results can be obtained in a more realistic simulation environment or reality. Employing time-varying

yaw actuation in active power control is, to the best of the authors knowledge, not employed yet. On the other hand, yaw actuation is employed for maximizing the wind farm power production. In fact, one of the first demonstrations of wake deflection due to a yawed turbine can be found in [10, 11]. Then in [12], the authors propose to utilize yaw control in a wind farm such that the wake is deflected in a way that mitigates wake impact on the wind farm performance. The authors in [13] illustrate that this methodology can increase the wind farm power production with respect to greedy control when evaluating and applying time-varying yaw settings that are found employing an adjoint based predictive controller.

A reference tracking solution is proposed in which a model predictive controller (MPC) solves a constrained optimization problem containing turbine models at each time step. These models are updated every measurement using the local rotor-averaged wind velocity that depend on the turbine settings of upstream turbines. The applied reference signal distribution is based on the yet to be defined instantaneous available power. This results in good tracking performance for reference signals below the averaged power harvested with greedy control settings. However, reference signals that are above this limit for a certain time will not be satisfactorily tracked. For these specific cases, the steady-state wind farm model FLORIS [14] is employed to find the optimal steady-state yaw angles that increase the available power in the farm using a wind direction measurement. The proposed general closed-loop control framework in depicted in Fig. 1.

In this paper, the proposed control frame work is evaluated for one case study in a high-fidelity simulation environment considering a six turbine wind farm case study. It is organised as follows. In Section 2, the high-fidelity simulation model will be introduced. In Section 3, the dynamical models that are employed in the controller are introduced and in Section 4, the controller itself is introduced. Then in Section 5, simulation results are presented and this paper is concluded in Section 6.

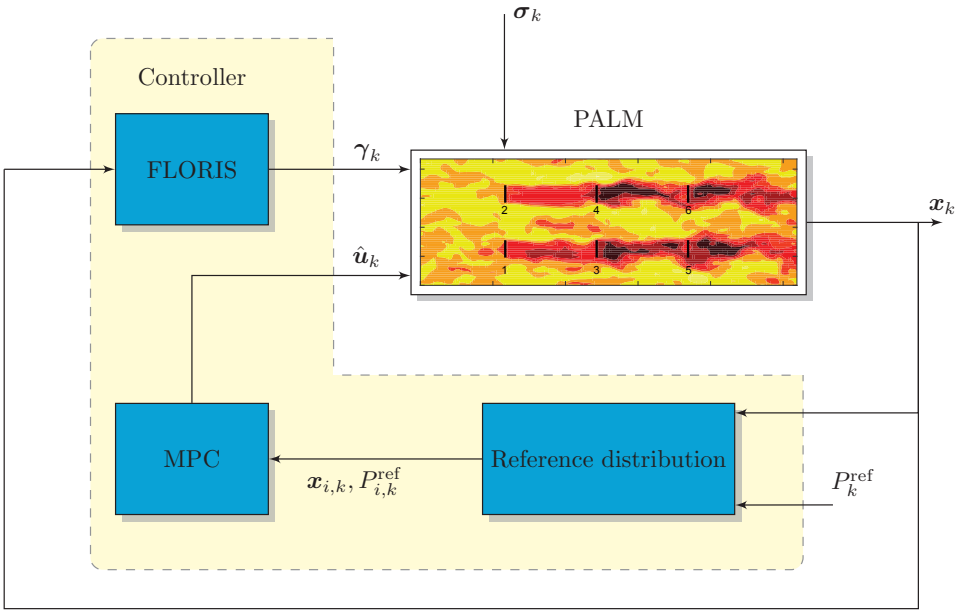

Figure 1: General idea of the closed-loop control framework with measurements $\boldsymbol{x}_k$. The signals P_k^{ref} and $P_{i,k}^{\text{ref}}$ are power reference signals for the farm and individual turbines, respectively. The control signals are the filtered thrust coefficients $\hat{\boldsymbol{u}}_k$ and yaw angels $\boldsymbol{\gamma}_k$ and $\boldsymbol{\sigma}_k$ the external wind farm perturbation such as, *e.g.*, boundary conditions.

2. Simulation model

The simulation model employed in this work is the PArallelized Large-eddy simulation Model (PALM) [15]. The PALM model is based on the filtered incompressible Navier-Stokes equations. In this work it includes the actuator disk model (ADM) to determine the turbine's forcing terms acting on the flow. This turbine model is efficient due its lower requirements of grid resolution and coarser allowed time-stepping as compared to having to resolve detailed flow surrounding rotating blades [16]. A consequence of choosing the ADM is that the control signals are the disk-based thrust coefficient $C'_{T_i}(t)$ following [16, 17]. Simulations are initialized as follows: a fully developed flow field is generated in the precursor with free-stream wind velocities U_∞=8 [m/s] and V_∞=W_∞=0 [m/s] in the x, y and z-direction respectively and a TI_∞ of approximately 6% at hub-height in front of the wind farm. Then, for the specific topology considered in this work, the flow is propagated 900 seconds in advance with constant control settings so that the wakes are fully developed. Here, non-cyclic boundary conditions and time-dependent turbulent inflow data are imposed by using a turbulence recycling method [15]. The flow field obtained after these 900 seconds is utilized as initial flow field (see Fig. 2) for the simulation results presented in this work. We assume that the measured variables at time t are 1) the force that a turbine exerts on the flow $F_i(t)$, 2) the power generated by a turbine $P_i(t)$ and 3) the rotor-averaged wind velocity $v_i(t)$ for $i = 1, 2, \ldots, \aleph$ with $\aleph$ the number of turbines in the farm. The rotor-averaged wind velocity is in this work assumed to be measured, but could be realized by employing online estimation of the rotor-averaged wind velocity with techniques as presented in [18, 19]. This is however outside the scope of this paper.

3. Controller model

A model predictive controller (MPC) is based on the receding horizon principle in which a finite-time constrained optimization problem is solved at each time step using future predictions of the system's state. However, due to nonlinear dynamics and uncertain atmospheric conditions, it is challenging to obtain a dynamical wind farm model suitable for online control. In this work we therefore employ wind turbine models with varying dynamical system parameters, since the measured rotor-averaged wind velocity is a time-varying parameter. This avoids the challenge of including a wake model in the optimization problem. The turbine models employed in the controller are based on the actuator disk theory:

$$P_i(t) = \frac{\pi D^2}{8}\Big(v_i(t)\cos[\gamma_i(t)]\Big)^3 \hat{u}_i(t), \qquad F_i(t) = \frac{\pi D^2}{8}\Big(v_i(t)\cos[\gamma_i(t)]\Big)^2 \hat{u}_i(t), \tag{1}$$

$$\tau\frac{\mathrm{d}\hat{u}_i(t)}{\mathrm{d}t} + \hat{u}_i(t) = u_i(t), \tag{2}$$

for $i = 1, 2, \ldots, \aleph$, with $P_i(t)$ the generated power and $F_i(t)$ the axial force belonging to turbine i, $u_i(t) = C'_{T_i}(t)$ the control signal, $\hat{u}_i(t)$ the first-order filtered control signal, $\gamma_i(t)$ the yaw angle and $v_i(t)$ the rotor-averaged longitudinal wind velocity, capturing the wake interaction between the turbines. We furthermore have $\tau \in \mathbb{R}^+$, the time constants of the filter that acts on the control signal. Temporally discretizing (2) at sample period Δt using the zero-order hold method, and lifting the state variables of the turbines results in the following state-space model:

$$\boldsymbol{x}_{k+1} = A\boldsymbol{x}_k + B(\boldsymbol{v}_k, \boldsymbol{\gamma}_k)\boldsymbol{u}_k, \quad \boldsymbol{y}_k = \boldsymbol{x}_k, \tag{3}$$

which is a linear parameter-varying system due to the matrix $B(\boldsymbol{v}_k, \boldsymbol{\gamma}_k)$, which changes according to each measured rotor-averaged wind velocity. Furthermore we have:

$$\boldsymbol{x}_k = \begin{pmatrix} \boldsymbol{x}_{1,k} \\ \boldsymbol{x}_{2,k} \\ \vdots \\ \boldsymbol{x}_{\aleph,k} \end{pmatrix} \in \mathbb{R}^{3\aleph}, \qquad \boldsymbol{x}_{i,k} = \begin{pmatrix} F_{i,k} \\ P_{i,k} \\ \hat{u}_{i,k} \end{pmatrix} \in \mathbb{R}^3, \quad A = \texttt{blkdiag}\Big(A_1, A_2, \dots, A_\aleph\Big) \in \mathbb{R}^{3\aleph \times 3\aleph},$$

$$\boldsymbol{u}_k, \hat{\boldsymbol{u}}_k \in \mathbb{R}^{\aleph}, \quad B(\boldsymbol{v}_k) = \texttt{blkdiag}\Big(B_1(v_{1,k}, \gamma_{1,k}), B_2(v_{2,k}, \gamma_{2,k}), \dots, B_\aleph(v_{\aleph,k}, \gamma_{\aleph,k})\Big) \in \mathbb{R}^{3\aleph \times \aleph},$$

where $\texttt{blkdiag}(\cdot)$ denotes block diagonal concatenation of matrices or vectors A_i and $B_i(v_{i,k}, \gamma_{i,k})$, respectively, for $i = 1, 2, \dots, \aleph$.

4. Control strategy

As described in the introduction, two steps can be distinguished in the controller. Firstly, the overall wind farm power reference needs to be divided among the turbines and secondly, control inputs need to be found such that performance specifications are met. The former will be discussed in §4.1 and the latter in §4.2.

4.1. Reference distribution

The following reference distribution is employed and based on work presented in [20]:

$$P_{i,k}^{\text{ref}} = \min\left(\frac{P_k^{\text{ref}}}{\sum_{i=1}^{\aleph} P_{i,k}^{\text{av}}} P_{i,k}^{\text{av}} \ , \ P_{i,k}^{\text{av}} \right), \quad P_{i,k}^{\text{av}} = \frac{\pi D^2}{8} \Big(v_{i,k} \cos[\gamma_{i,k}] \Big)^3 \overline{u}_i, \tag{4}$$

with $P_{i,k}^{\text{av}}$ the instantaneous available power for the i^{th} turbine, P_k^{ref} the wind farm power reference signal, $P_{i,k}^{\text{ref}}$ the reference signal for the i^{th} turbine and $\overline{u}_i = 2$ the maximum value of the control signals. Note that the definition for available power is different from literature such as [21] in which the free-stream wind velocity is first estimated from the rotor-averaged wind velocity so that the former is only a function of the upstream turbines. This estimation is then used in an optimization algorithm to estimate the therein defined possible power. In this work, $P_{i,k}^{\text{av}}$ is not only a function of the upstream turbine settings, but also of the settings of turbine i itself. This is due to the fact that a change in the control signal results in an alteration of the rotor-averaged flow velocity $v_{i,k}$ that consequently changes the $P_{i,k}^{\text{av}}$. Additionally, $v_{i,k}$ can of course also vary due to changes in the upstream turbine settings. An advantage of employing (4) is that only the rotor-averaged flow velocity is assumed to be measured and no additional estimation of the free-stream wind velocity and other approximations are required.

4.2. Model Predictive Controller

The MPC, for which stability and performance can be ensured [22], solves the following optimization problem at time k_0 until the prediction horizon N_h:

$$\min_{\boldsymbol{u}_k} \quad \sum_{k=k_0}^{k_0+N_h} (\boldsymbol{x}_k - \boldsymbol{x}_k^{\text{ref}})^T Q (\boldsymbol{x}_k - \boldsymbol{x}_k^{\text{ref}}) + \boldsymbol{u}_k^T R \boldsymbol{u}_k + (\boldsymbol{x}_k - \boldsymbol{x}_{k-1})^T S (\boldsymbol{x}_k - \boldsymbol{x}_{k-1}), \tag{5a}$$

$$\text{s.t.} \quad \boldsymbol{x}_{k+1} = A\boldsymbol{x}_k + B(\boldsymbol{v}_{k_0}, \boldsymbol{\gamma}_{k_0})\boldsymbol{u}_k, \quad \underline{\boldsymbol{x}} \le \boldsymbol{x}_k \le \overline{\boldsymbol{x}}, \quad \underline{u} \le \boldsymbol{u}_k \le \overline{u}, \quad |\boldsymbol{u}_k - \boldsymbol{u}_{k-1}| < \mathrm{d}\overline{u}, \tag{5b}$$

where $\overline{u} = 2, \underline{u} = 0$, $\mathrm{d}\overline{u} = 1/5$ and $\overline{\boldsymbol{x}}, \underline{\boldsymbol{x}}$ represent the maximum and minimum bounds on the control variables, its variation and state (force and power), respectively, and $\boldsymbol{x}_{k_0}$ and $\boldsymbol{v}_{k_0}$ the

measured state and rotor-averaged wind velocity at time k_0, respectively. We furthermore have the weighting matrices:

$$R = I_{\aleph} \cdot r \in \mathbb{R}^{\aleph \times \aleph}, \qquad Q = I_{\aleph} \otimes \begin{pmatrix} 0 & 0 & 0 \\ 0 & q & 0 \\ 0 & 0 & 0 \end{pmatrix} \in \mathbb{R}^{3\aleph \times 3\aleph}, \qquad S = I_{\aleph} \otimes \begin{pmatrix} s & 0 & 0 \\ 0 & 0 & 0 \\ 0 & 0 & 0 \end{pmatrix} \in \mathbb{R}^{3\aleph \times 3\aleph},$$

with $\otimes$ the Kronecker product and $r, q, s \in \mathbb{R}$ controller tuning variables. More precisely, by tuning each weight one can increase or decrease the importance of tracking error, control signal and variation in the force, respectively. In addition:

$$\begin{aligned} \boldsymbol{x}_k^{\text{ref}} &= \begin{pmatrix} 0 & P_{1,k}^{\text{ref}} & 0 & 0 & P_{2,k}^{\text{ref}} & 0 & \dots & 0 & P_{\aleph,k}^{\text{ref}} & 0 \end{pmatrix}^T \in \mathbb{R}^{3\aleph}, \\ \overline{\boldsymbol{x}} &= \begin{pmatrix} F_{1,k_0}^{\max} & P_{1,k_0}^{\text{av}} & 2 & F_{2,k_0}^{\max} & P_{2,k_0}^{\text{av}} & 2 & \dots & F_{\aleph,k_0}^{\max} & P_{\aleph,k_0}^{\text{av}} & 2 \end{pmatrix}^T \in \mathbb{R}^{3\aleph} \\ \underline{\boldsymbol{x}} &= \begin{pmatrix} 0 & 0 & 0 & 0 & 0 & 0 & \dots & 0 & 0 & 0 \end{pmatrix}^T \in \mathbb{R}^{3\aleph}, \end{aligned}$$

and $F_{i,k_0}^{\max} = \pi D^2/8(v_{i,k_0}\cos[\gamma_{i,k_0}])^2\overline{u}_i$. Note that a constraint on the axial force is an indirect constraint on the control signal since, during the prediction horizon, only the decision variable $\boldsymbol{u}_k$ can be varied. However, the general formulation above allows us to research in possible future work the effect of imposing, *i.e.*, different axial force constraints on each turbine.

5. Simulation results

The PALM simulation results are all of a neutral atmospheric boundary layer and will be discussed in this section. Firstly, in §5.2, a simulation case is presented in which the controller is working under yawed conditions that, as will be shown, increases the set of trackable wind farm reference signals. In §5.3, we study the effect of the controller on the variation of the axial force. In all cases, the controller is applied to a wind farm with specifications as described in Table 1. See Fig. 2 for the initial longitudinal flow field at hub height. Note that the topology under consideration contains heavily waked wind turbines due to the fact that turbines are aligned with the mean wind direction. Although farms are designed such that the occurrence of this situation is minimized, it remains an interesting case study to investigate farm dynamics in these worst case scenarios.

Table 1: Summary of the simulation set-up.

$L_x \times L_y \times L_z$	$15.3 \times 3.8 \times 1.3$ [km^3]	D, z_h	120, 90 [m]
$\Delta x \times \Delta y \times \Delta z$	$15 \times 15 \times 10$ [m^3]	Turbine spacing	$5D \times 3D$ [m]
Δt	1 [s]	$U_\infty, V_\infty, W_\infty$	$8, 0, 0$ [m/s]
N, τ, N_h	900,5,10 [s]	TI_∞,	6%

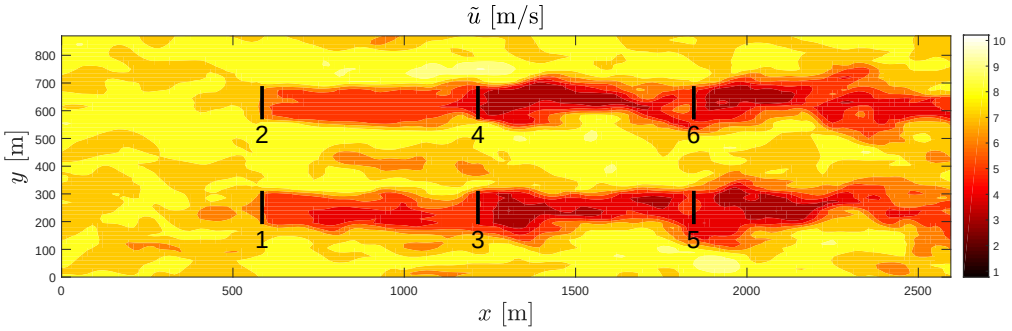

Figure 2: Initial longitudinal flow velocity component at hub-height. The flow is going from west to east and the black vertical lines represent the wind turbines.

5.1. Performance measures

In order to evaluate the controller performance under different settings, two criteria are introduced.

$$||e_k||_2 = \left(\frac{||P_k^{\text{ref}} - \sum_{i=1}^{\aleph} P_{i,k}||_2}{e_{\text{base}}} - 1 \right) \cdot 100\ \%, \quad \text{d}F_i = \left(\frac{\sum_{k=1}^{N} (F_{i,k} - F_{i,k-1})^2}{dF_{i,\text{base}}} - 1 \right) \cdot 100\ \%, \quad (6)$$

with $dF_{i,\text{base}} = \sum_{k=1}^{N} (F_{i,k} - F_{i,k-1})^2$ and $e_{\text{base}} = ||P_k^{\text{ref}} - \sum_{i=1}^{\aleph} P_{i,k}||_2$ for $s = 0$. Note that a negative $||e_k||_2$ indicates improved tracking and a negative $\text{d}F_i$ indicates decreased force variations over the complete simulation time with respect to the $s = 0$ case.

5.2. Active power control with different yaw settings

In this section, the proposed MPC is evaluated under zero yaw and yaw settings for maximal power capture in steady-state. The wind farm power reference signal is defined as:

$$P_k^{\text{ref}} = 0.8 P^{\text{greedy}} + 0.3 P^{\text{greedy}} \delta P_k, \quad (7)$$

with δP_k a normalized "RegD" type AGC signal [23] coming from an operator, and $P^{\text{greedy}} \approx 7.5$ [MW] the time-averaged produced wind farm power under greedy control, *i.e.*, with $u_{i,k} = 2$ and $\gamma_{i,k} = 0$ over the complete simulation horizon. Note that, for a short period, more power is demanded from the farm than the averaged power harvested under greedy control. The simulation results are obtained with controller parameters $q = 10^4, r = 10^3, s = 0$ that are found after tuning and are presented in Fig. 3. The top plot in Fig. 3 illustrates that the power reference can not be tracked without an undesired error for a period between 300 and 600 seconds. This is due to a demanded power larger than the previously defined available power in the farm under the imposed reference distribution (see (4)). The authors in [24] already illustrate that redirecting the wake can be beneficial during active power control when demanding more power from the farm than available under non-yawed turbines. Following this idea, optimal steady-state yaw settings are imposed during the complete simulation. These settings, $\boldsymbol{\gamma}_k = \boldsymbol{\gamma}_k^* = (\text{-}24.3\ \text{-}24.3\ \text{-}16.2\ \text{-}16.2\ 0\ 0)^T$ [deg], are found using the wind farm optimization tool FLORIS [25]. In here, the steady-state wind farm model FLORIS is utilized to predict and maximize the steady-state power production for different yaw settings. The bottom plot of Fig. 3 illustrates that better tracking is ensured when the turbines are set to their optimal yaw settings with respect to the case when $\gamma_{i,k} = 0$. This is due to the increase of available power when controlling under optimal yaw settings and consequently, reference signals with higher amplitudes can be tracked. Instead of yawing the turbines, it could also be possible to increase the available power by imposing a different distribution than presented in (4). This

idea is however not further investigated in this work. The tracking results of the individual turbines can be found in Fig. 4 and Fig. 5 and the control signals of the yawed case in Fig. 6.

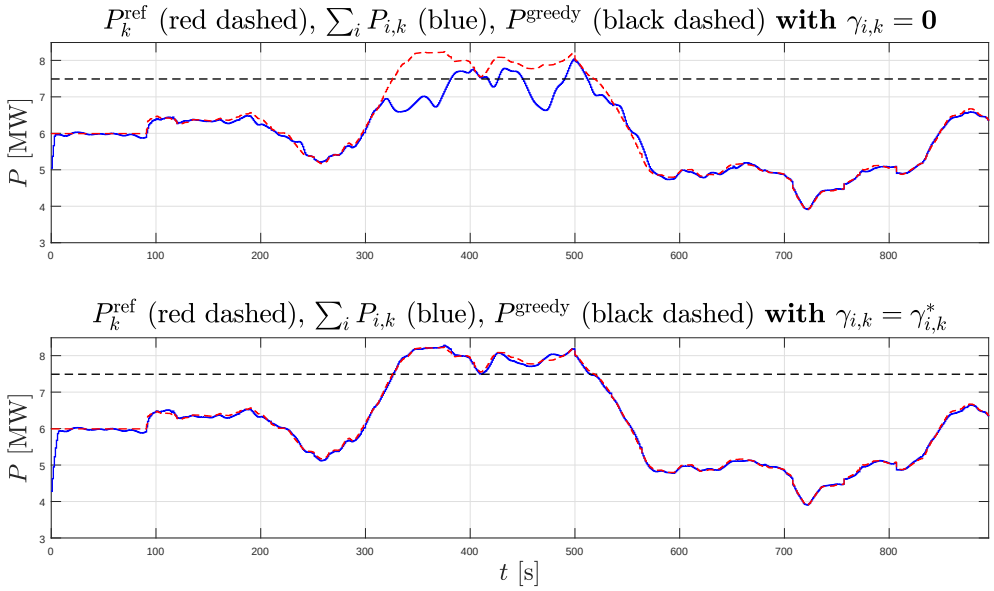

Figure 3: Wind farm tracking results of the controller with $\gamma_{i,k} = 0$ (above) and optimized settings $\boldsymbol{\gamma}_k^* = (\text{-}24.3\ \text{-}24.3\ \text{-}16.2\ \text{-}16.2\ 0\ 0)^T$ [deg] (below).

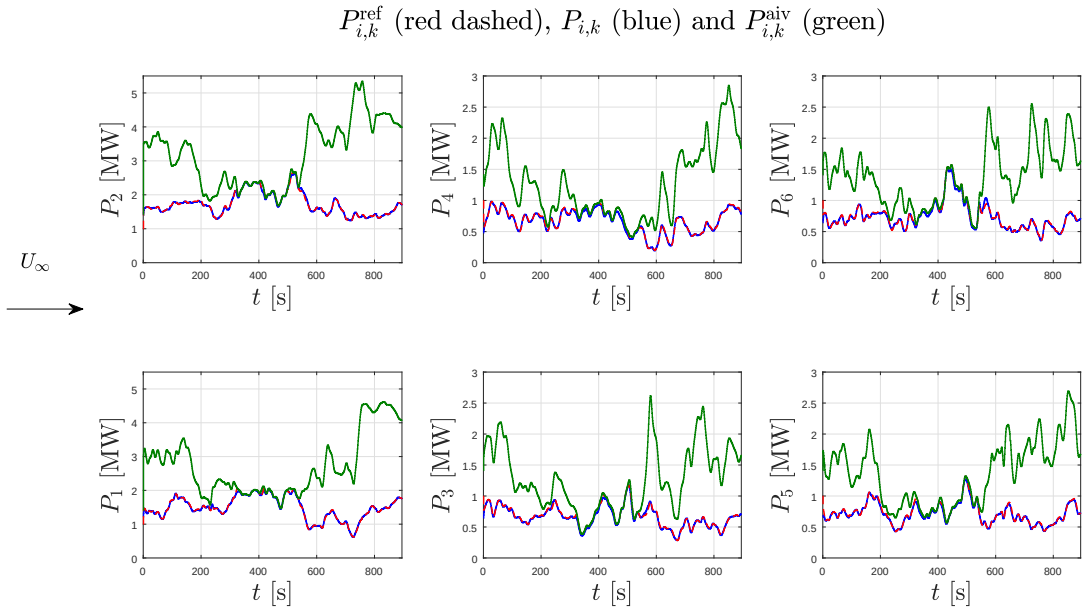

Figure 4: Turbine tracking results of the controller with $\gamma_{i,k} = 0$. The black arrow on the left of the figure indicates the wind direction.

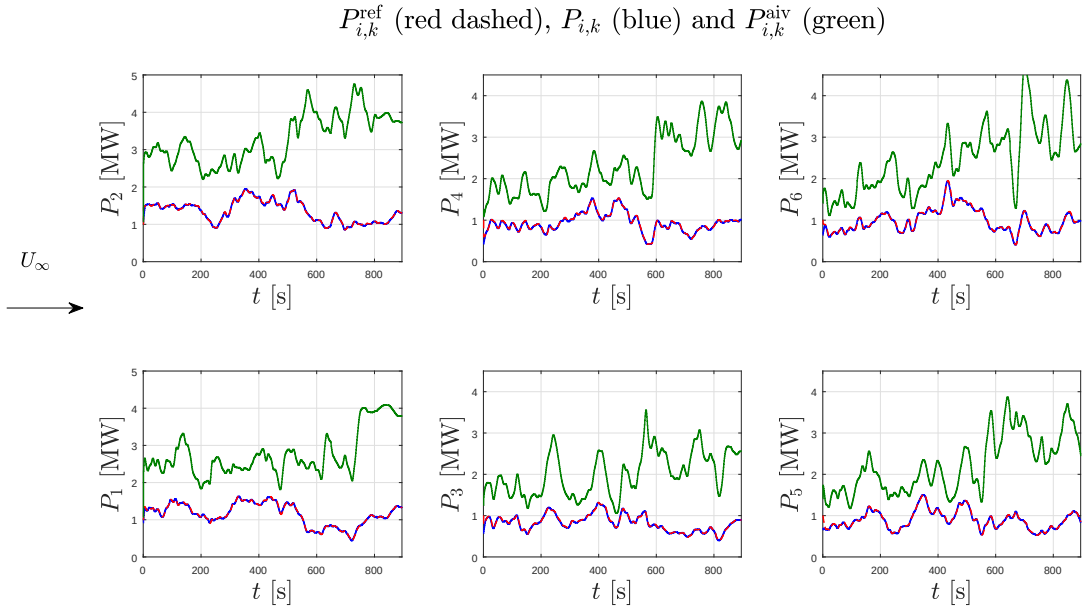

Figure 5: Turbine tracking results of the controller with $\boldsymbol{\gamma}_k^* = (\text{-}24.3\ \text{-}24.3\ \text{-}16.2\ \text{-}16.2\ 0\ 0)^T$ [deg]. The black arrow on the left of the figure indicates the wind direction.

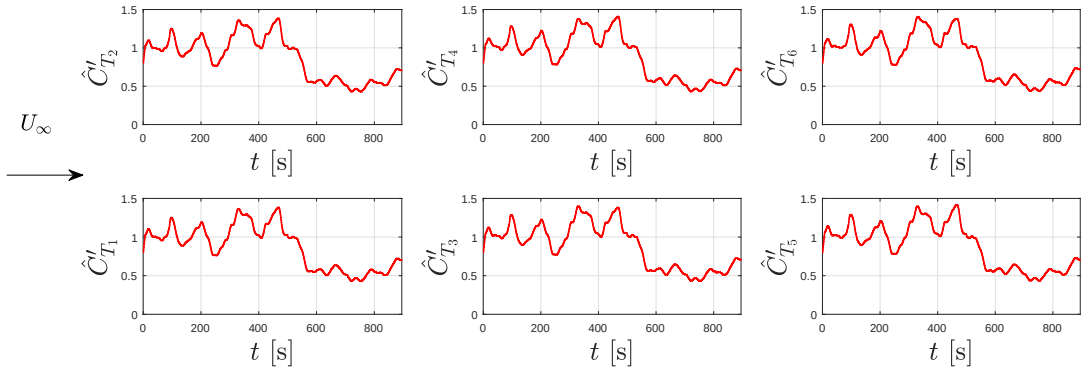

Figure 6: Turbine thrust coefficients with $\boldsymbol{\gamma}_k^* = (\text{-}24.3\ \text{-}24.3\ \text{-}16.2\ \text{-}16.2\ 0\ 0)^T$ [deg]. Note that the control signals are similar though not equivalent.

5.3. Active power control while minimizing the axial force variation

This section studies the effect of the controller tuning parameter s (see (5)). This weight acts on the axial force variation and an increasing s makes the optimization penalize the variation in the force more. One could consider this variation as a measure for turbine fatigue and it is therefore interesting to minimize this quantity, possibly expanding the turbine's lifetime. The following wind farm power reference signal is applied:

$$P_k^{\text{ref}} = 0.7P^{\text{greedy}} + 0.2P^{\text{greedy}}\delta P_k. \tag{8}$$

Note that here, the reference signal is not exceeding greedy power, which makes it an less challenging tracking task than presented in Section 5.2. In total, four simulations are performed with each a different value for s, but under constant $q = 10^4, r = 10^3$ that are found after tuning

the controller. Table 2 gives the performance measures that corresponds to the different values of the weight s.

Table 2: Weight s on the variation of the force, with corresponding performance measures as given in (6). During all simulation scenarios presented here we have $\gamma_{i,k} = 0$.

s	$\|\|e_k\|\|_2$ [%]	dF_1 [%]	dF_2 [%]	dF_3 [%]	dF_4 [%]	dF_5 [%]	dF_6 [%]
50	0.94	-4.38	-1.82	-2.26	1.89	-2.43	1.82
250	-2.91	-1.95	-2.22	-0.91	-0.14	-5.94	5.28
500	1.06	-4.42	-1.86	-2.29	1.86	-2.44	1.78
1000	-2.72	-2.01	-2.28	-0.97	-0.18	-5.96	5.23

From Table 2 it can be concluded that an increasing weight s results in an overall decrease in the force variation over the complete simulation horizon, which is expected and desired since the penalty on this quantity is increased. An additional consequence is the relatively small change in the tracking behaviour.

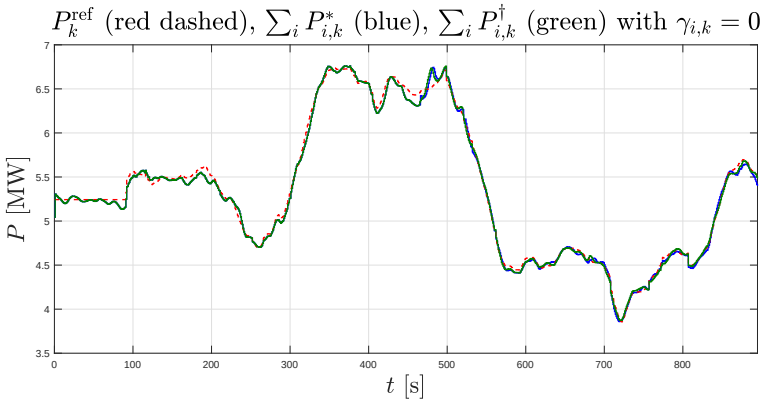

Figure 7: Wind farm tracking results of the MPC for two different weights s. The power signal $\sum_i P_{i,k}^*$ is obtained with $s^* = 0$ and $\sum_i P_{i,k}^\dagger$ with $s^\dagger = 10^3$.

6. Conclusions

We developed and tested a constrained model predictive controller (MPC) in the high-fidelity PArallelized Large-eddy simulation Model (PALM). The MPC provides secondary frequency regulation while minimizing axial force variations using the thrust coefficient. It has been illustrated that a wind farm power reference signal that exceeds for a certain period the averaged greedy power, tracking can not be ensured. Therefore, an additional loop has been proposed that takes the current wind direction and optimizes for yaw settings such that the available power increases and consequently, a broader class of reference signals can be tracked. This has been illustrated in one case study. Additionally, different controller settings are compared. During each forward prediction in the MPC, the instantaneous available power is considered constant although this quantity depends on the power production of upstream and local turbine settings. This dependency is not taken into account in the optimization, but could be included by incorporating a wake model in the MPC.

Acknowledgements
The main author would like to thank Sonja Krüger and Gerald Steinfeld from ForWind (Oldenburg) for their valuable input regarding the PALM simulations.

References

[1] B. Obama, "The irreversible momentum of clean energy," *Science Policy Forum*, 2017.
[2] E. Ela, V. Gevorgian, P. A. Fleming, Y. C. Zhang, M. Singh, E. Muljadi, A. Scholbrock, J. Aho, A. Buckspan, L. Y. Pao, V. Singhvi, A. Tuohy, P. Pourbeik, D. Brooks, and N. Bhatt, "Active power controls from wind power: Bridging the gaps," technical report, National Renewable Energy Laboratory, 2014.
[3] S. Boersma, B. M. Doekemeijer, P. M. O. Gebraad, P. A. Fleming, J. Annoni, A. K. Scholbrock, J. A. Frederik, and J. W. van Wingerden, "A tutorial on control-oriented modelling and control of wind farms," *American Control Conference*, 2017.
[4] C. R. Shapiro, P. Bauweraerts, J. Meyers, C. Meneveau, and D. F. Gayme, "Model-based receding horizon control of wind farms for secondary frequency regulation," *Wind Energy*, 2017.
[5] J. W. van Wingerden, L. Y. Pao, J. Aho, and P. A. Fleming, "Active power control of waked wind farms," *International Federation of Automatic Control*, 2017.
[6] S. Siniscalchi-Minna, F. D. Bianchi, and C. Ocampo-Martinez, "Predictive control of wind farms based on lexicographic minimizers for power reserve maximization," *American Control Conference*, 2018.
[7] V. Spudić, M. Jelavić, M. Baotić, and N. Perić, "Hierarchical wind farm control for power/load optimization," *Journal of Physics: Conference Series*, 2010.
[8] D. Madjidian, K. Mortensson, and A. Rantzer, "A distributed power coordination scheme for fatigue load reduction in wind farms," *American Control Conference*, 2011.
[9] B. Biegel, D. D. Madjidian, V. Spudić, A. Rantzer, and J. Stoustrup, "Distributed low-complexity controller for wind power plant in derated operation," *International Conference on Control Applications*, 2013.
[10] B. Clayton and P. Filby, "Measured effects of oblique flows and change in blade pitch angle on performance and wake development of model wind turbines," *BWEA Wind Energy Conference*, 1982.
[11] B. Grant, P. Parkin, and X. Wang, "Optical vortex tracking studies of a horizontal axis wind turbine in yaw using laser-sheet, flow visualisation," *Experiments in Fluids*, 1997.
[12] Á. Jiménez, A. Crespo, and E. Migoya, "Application of a LES technique to characterize the wake deflection of a wind turbine in yaw," *Wind Energy*, 2010.
[13] W. Munters and J. Meyers, "Dynamic strategies for yaw and induction control of wind farms based on large-eddy simulation and optimization," *Energies*, 2018.
[14] P. M. O. Gebraad, F. W. Teeuwisse, J. W. van Wingerden, P. A. Fleming, S. D. Ruben, J. R. Marden, and L. Y. Pao, "Wind plant power optimization through yaw control using a parametric model for wake effects - a CFD simulation study," *Wind Energy*, 2014.
[15] B. Maronga, M. Gryschka, R. Heinze, F. Hoffmann, F. Kanani-Sühring, M. Keck, K. Ketelsen, M. O. Letzel, M. Sühring, and S. Raach, "The Parallelized Large-Eddy Simulation Model (PALM) version 4.0 for atmospheric and oceanic flows: model formulation, recent developments, and future perspectives," *Geoscientific Model Development*, 2015.
[16] J. Meyers and C. Meneveau, "Large Eddy Simulations of large wind-turbine arrays in the atmospheric boundary layer," *Aerospace Sciences Meeting*, 2010.
[17] S. Boersma, B. M. Doekemeijer, M. Vali, J. Meyers, and J. W. van Wingerden, "A control-oriented dynamic wind farm model: WFSim," *Wind Energy Science*.
[18] C. R. Shapiro, J. Meyers, C. Meneveau, and D. F. Gayme, "Dynamic wake modeling and state estimation for improved model-based receding horizon control of wind farms," *American Control Conference*, 2017.
[19] B. M. Doekemeijer, S. Boersma, L. Y. Pao, T. Knudsen, and J. W. van Wingerden, "Online model calibration for a simplified les model in pursuit of real-time closed-loop wind farm control," *Wind Energy Science Discussions*, 2018.
[20] A. D. Hansen, P. Sørensen, F. Iov, and F. Blaabjerg, "Centralised power control of wind farm with doubly fed induction generators," *Renewable Energy*, 2006.
[21] T. Göçmen, G. Giebel, J. E. Sørensen, and N. K. Poulsen, *Possible Power Estimation of Down-Regulated Offshore Wind Power Plants.* PhD thesis, Technical University of Denmark, 2016.
[22] D. Q. Mayne, J. B. Rawlings, C. V. Rao, and P. O. Scokaert, "Constrained model predictive control: Stability and optimality," *Automatica*, 2000.
[23] C. Pilong, "PJM Manual 12: Balancing Operations," technical report, PJM, 2013.
[24] P. A. Fleming, J. Aho, P. M. O. Gebraad, L. Y. Pao, and Y. Zhang, "Computational fluid dynamics simulation study of active power control in wind plants control in wind plants," *American Control Conference*, 2016.
[25] github.com/TUDelft-DataDrivenControl/FLORISSE_M.